NeuroImage 90 (2014) 246–255

Contents lists available at ScienceDirect

NeuroImage

journal homepage: www.elsevier.com/locate/ynimg

Different topological organization of human brain functional networks with eyes open versus eyes closed

Pengfei Xu [a], Ruiwang Huang [a,b,*], Jinhui Wang [a], Nicholas T. Van Dam [c], Teng Xie [a], Zhangye Dong [a], Chunping Chen [d], Ruolei Gu [e], Yu-Feng Zang [a,f], Yong He [a,g], Jin Fan [h,i,j,k], Yue-jia Luo [l,**]

[a] State Key Laboratory of Cognitive Neuroscience and Learning, Beijing Normal University, Beijing 100875, China
[b] Brain Imaging Center, Center for Studies of Psychological Application, Guangdong Key Laboratory of Mental Health and Cognitive Science, School of Psychology, South China Normal University, Guangzhou 510631, China
[c] Department of Psychiatry, New York University School of Medicine, New York, NY 10016, USA
[d] Key Laboratory of Mental Health, Institute of Psychology, Chinese Academy of Sciences, Beijing 100101, China
[e] Key Laboratory of Behavioral Science, Institute of Psychology, Chinese Academy of Sciences, Beijing 100101, China
[f] Center for Cognition and Brain Disorders, Affiliated Hospital, Hangzhou Normal University, Hangzhou 310015, China
[g] IDG/McGovern Institute for Brain Research, Beijing Normal University, Beijing 100875, China
[h] Department of Psychology, Queens College, The City University of New York, New York, NY 11367, USA
[i] Department of Psychiatry, Ichan School of Medicine at Mount Sinai, New York, NY 10029, USA
[j] Fishberg Department of Neuroscience, Ichan School of Medicine at Mount Sinai, New York, NY 10029, USA
[k] Friedman Brain Institute, Ichan School of Medicine at Mount Sinai, New York, NY 10029, USA
[l] Institute of Affective and Social Neuroscience, Shenzhen University, Shenzhen 518060, China

ARTICLE INFO

Article history:
Accepted 30 December 2013
Available online 13 January 2014

Keywords:
Exteroceptive
Interoceptive
Connectome
Graph theory
Resting-state functional MRI

ABSTRACT

Opening and closing the eyes are fundamental behaviors for directing attention to the external versus internal world. However, it remains unclear whether the states of eyes-open (EO) relative to eyes-closed (EC) are associated with different topological organizations of functional neural networks for exteroceptive and interoceptive processing (processing the external world and internal state, respectively). Here, we used resting-state functional magnetic resonance imaging and neural network analysis to investigate the topological properties of functional networks of the human brain when the eyes were open versus closed. The brain networks exhibited higher cliquishness and local efficiency, but lower global efficiency during the EO state compared to the EC state. These properties suggest an increase in specialized information processing along with a decrease in integrated information processing in EO (vs. EC). More importantly, the "exteroceptive" network, including the attentional system (e.g., superior parietal gyrus and inferior parietal lobule), ocular motor system (e.g., precentral gyrus and superior frontal gyrus), and arousal system (e.g., insula and thalamus), showed higher regional nodal properties (nodal degree, efficiency and betweenness centrality) in EO relative to EC. In contrast, the "interoceptive" network, composed of visual system (e.g., lingual gyrus, fusiform gyrus and cuneus), auditory system (e.g., Heschl's gyurs), somatosensory system (e.g., postcentral gyrus), and part of the default mode network (e.g., angular gyrus and anterior cingulate gyrus), showed significantly higher regional properties in EC vs. EO. In addition, the connections across sensory modalities were altered by volitional eye opening. The synchronicity between the visual system and the motor, somatosensory and auditory systems, characteristic of EC, was attenuated in EO. Further, the connections between the visual system and the attention, arousal and subcortical systems were increased in EO. These results may indicate that EO leads to a suppression of sensory modalities (other than visual) to allocate resources to exteroceptive processing. Our findings suggest that the topological organization of human brain networks dynamically switches corresponding to the information processing modes as we open or close our eyes.

Introduction

While vision has featured centrally in prominent scientific theories of consciousness (Crick and Koch, 2003), we spend a considerable portion of our lives with our eyes closed, thereby attenuating the potential contributions of vision. Interestingly, a recent study suggested that momentary closing of the eyes (blinking) not only occurs more often than would be necessary for ocular lubrication, but that these blinks are

* Correspondence to: Ruiwang Huang, Centre for Studies of Psychological Application, Guangdong Key Laboratory of Mental Health and Cognitive Science, School of Psychology, South China Normal University, Guangzhou 510631, China. Fax: +86 20 8521 6499.
** Correspondence to: Yue-jia Luo, Institute of Affective and Social Neuroscience, Shenzhen University, Shenzhen 518060, China. Fax: +86 10 58802365.
E-mail addresses: ruiwang.huang@gmail.com (R. Huang), luoyj@bnu.edu.cn (Y. Luo).

1053-8119/$ – see front matter © 2014 Published by Elsevier Inc.
http://dx.doi.org/10.1016/j.neuroimage.2013.12.060

associated with subtle shifts in neural activity (Nakano et al., 2013). While awake, awareness shifts based on whether our eyes are open or closed; awareness has been described as "exteroceptive" when the eyes are open (EO) and "interoceptive" when the eyes are closed (EC). These states correspond to focus on the "outside" versus the "inside", respectively, and each has different psychophysiological characteristics and underlying brain mechanisms (Marx et al., 2003).

Compared to EC, an increased attentional load and raised level of arousal is present in EO (Hufner et al., 2009). The differences attributable to these states may have more to do with the simple processing of visual information; even in the darkness, where little to no visual input is present, these two states reveal distinct neural activation patterns (Hufner et al., 2009). Attentional and oculomotor systems (e.g., superior parietal gyrus and frontal eye fields) show activation in EO, while sensory systems (e.g., visual, auditory, and somatosensory) show activation in EC (Bianciardi et al., 2009; Hufner et al., 2008, 2009; Marx et al., 2003, 2004; McAvoy et al., 2008; Niven and Laughlin, 2008). These findings suggest two different states of mental activity: an "exteroceptive" state characterized by overt attention and ocular motor activity (during EO) and an "interoceptive" state characterized by imagination and multisensory activity (during EC) (Hufner et al., 2009; Marx et al., 2004). The corresponding differences of spontaneous neural activity between these two states have been characterized in previous resting-state functional magnetic resonance imaging (R-fMRI) studies (Bianciardi et al., 2009; McAvoy et al., 2008; Yan et al., 2009; Yang et al., 2007; Zou et al., 2009).

More recently, an R-fMRI study, by manipulating both eyes open/closed and lights on/off, found that there were significant differences between EO and EC in both spontaneous brain activity and functional connectivity but no differences in whole brain topological organization other than connection distance (i.e., the Euclidean distance between each pair of regional nodes) (Jao et al., 2013). Given that the topological properties of human brain networks have shown correlations with various cognitive functions and pathologies (Bullmore and Sporns, 2009; He and Evans, 2010), it is curious that there were widespread influences of EO and EC on the spontaneous activity and connectivity but not on the topological organization of the networks (Jao et al., 2013).

Given that there are critical influence of different acquisition parameters and analytic strategies in R-fMRI data but lacking consensus about the best way to deal with it (Murphy et al., 2009; Wang et al., 2009; Wig et al., 2011; Zuo et al., 2013), we acquired human R-fMRI data and constructed whole brain functional networks with different brain parcellation templates and presence/absence of global signal regression (GSR) to compare topological parameters (e.g., small-world, network efficiency and nodal efficiency) of brain networks between the EO and EC states. We hypothesized that the "exteroceptive" state and the "interoceptive" state were associated with different topological organizations of brain networks corresponding to different information processing modes. Specifically, we predicted that there would be an "exteroceptive" network, characterized by attention and ocular motor system during EO, and an "interoceptive" network characterized by imagination and multisensory system during EC.

Materials and methods

Subjects

Twenty-three right-handed healthy volunteers (11 females; mean age ± SD, 20.17 ± 2.74 years) participated in this study. All participants were undergraduate/graduate students and had no history of neurological and psychiatric disorders or head injury. Written informed consent was obtained from each participant prior to the MRI acquisition. The study was approved by the Institutional Review Board of Beijing Normal University.

Data acquisition

MRI data were acquired on a Siemens Trio 3 T MRI scanner powered with a total imaging matrix technique at the Imaging Center for Brain Research, at Beijing Normal University. Both the R-fMRI and high resolution 3D structural brain data were obtained using a 12-channel phased-array receiver-only head coil with the implementation of parallel imaging scheme GRAPPA (GeneRalized Autocalibrating Partially Parallel Acquisitions) (Griswold et al., 2002). For scanning, we selected the acceleration factor 2. The R-fMRI data were acquired using gradient-echo echo-planar imaging (EPI). The sequence parameters were as follows: TR = 3000 ms, TE = 30 ms, slice thickness = 3.5 mm with no gap, flip angle = 90°, FOV = 224 mm × 224 mm, data matrix = 64 × 64, interleaved 40 transversal slices giving spatial coverage 140 mm and 160 volumes. Each subject underwent the R-fMRI scans in two runs, EC state and EO state, each lasting 8 min. The order of the R-fMRI data acquisitions (corresponding to the two states) was counterbalanced across all subjects. In addition, we also acquired the 3D high-resolution brain structural images (1 mm^3 isotropic) for each subject using a T1-weighted MP-RAGE sequence. The sequence parameters were TR/TE = 1900 ms/3.44 ms, flip angle = 9°, data matrix = 256 × 256, FOV = 256 mm × 256 mm, BW = 190 Hz/pixel, and 176 images along sagittal orientation, obtained in about 6 min.

Data preprocessing

The data preprocessing was conducted using SPM8 (http://www.fil.ion.ucl.ac.uk/spm/) and DPARSF (Yan and Zang, 2010). For each subject, the two R-fMRI runs (EO and EC) were processed separately. For each run, the first 10 volumes were discarded to account for the MR signal equilibration. The remaining functional images were first corrected for timing, and then realigned to the first volume to correct for head motion, which did not exceed 2.0 mm of displacement or 2.0° of rotation in any direction, in any subject. To account for the influence of head motion on R-fMRI (Mowinckel et al., 2012; Power et al., 2012; Satterthwaite et al., 2012; Van Dijk et al., 2012), the root mean squares of both overall head displacement and head rotation were calculated under EO and EC, and no significant differences were found between EO and EC ($ps > 0.2$). Subsequently, the functional images were spatially normalized to the standard MNI-152 template and re-sampled to a voxel size of 3 × 3 × 3 mm^3. The waveform of each voxel was finally passed through a band-pass filter (0.01–0.08 Hz) to reduce the effects of low-frequency drift and high-frequency physiological noise.

Construction of brain functional networks

The functional connectivity matrix of each subject was constructed based on the automated anatomical labeling (AAL) (Tzourio-Mazoyer et al., 2002), which parcellated the brain into 90 regions of interest (ROIs; Table S1). The mean time series of each ROI was calculated by averaging the time series of all voxels within that ROI. The effects of head-motion profiles and global signal were regressed out with multiple linear regression analyses as described in previous studies (Fox et al., 2005; Van Dijk et al., 2012; Wang et al., 2009). Given that the impact of global signal regression (GSR) is important and its contributions, intensely debated (Chai et al., 2012b; Fox et al., 2009; Murphy et al., 2009; Van Dijk et al., 2010; Weissenbacher et al., 2009), we repeated the data analysis without GSR to check the reliability of the results (Supplementary materials). Regression residuals were then substituted for the raw mean time series of the corresponding ROIs. Pearson's correlation between the residual time series of each pair of the 90 ROIs was calculated to obtain a symmetric correlation matrix, the functional connectivity matrix for each subject. Finally, all elements of the correlation matrix were truncated and binarized by using a pre-selected value of sparsity (the ratio between total number of edges and the maximum possible number of edges in a network). To ensure that the brain

networks under EO and EC had the same number of edges, each correlation matrix was set to different thresholds over a specific range of sparsity (see the Results section), where prominent small-world properties in brain networks were observed (Watts and Strogatz, 1998b). For each given sparsity, we obtained an undirected binarized network, in which nodes represented brain regions and edges represented links between brain regions. Graph theory was then applied to analyze the topological organization of functional brain networks.

Network analysis

Global properties of functional brain networks

Graph theory can be used to characterize the brain functional networks quantitatively (Bullmore and Sporns, 2009; Hagmann et al., 2008; He and Evans, 2010). Here, six network parameters: clustering coefficient (C_p), characteristic path length (L_p), normalized clustering coefficient (γ), normalized shortest path length (λ), global efficiency (E_{glob}), and local efficiency (E_{loc}), were used to characterize the global topological properties of brain networks. The definitions and descriptions of C_p (Watts and Strogatz, 1998b), L_p (Newman, 2003), E_{glob} (Latora and Marchiori, 2001), and E_{loc} (Latora and Marchiori, 2001) can be found in the Appendix and in Rubinov and Sporns (2010).

The small-world property of a network can be characterized by both the normalized clustering coefficient $\gamma = \frac{C_p^{real}}{C_p^{rand}}$ and the normalized characteristic path length $\lambda = \frac{L_p^{real}}{L_p^{rand}}$ (Watts and Strogatz, 1998b). C_p^{real} and L_p^{rand} are the clustering coefficient and the characteristic path length of the real brain networks, and the C_p^{rand} and L_p^{rand} represent the mean indices derived from matched random networks (100 matched random networks were selected). The benchmark random networks were constructed in a way that preserved the same number of nodes, edges, and degree distribution as the real brain networks (Maslov and Sneppen, 2002; Milo et al., 2002). Considering that correlation networks are inherently more clustered than the nodes and degree matched random networks, the Hirschberger–Qi–Steuer algorithm (H–Q–S; Zalesky et al., 2012) was performed to verify the results. Typically, a small-world network should meet the following criteria: $\gamma > 1$ and $\lambda \approx 1$ (Watts and Strogatz, 1998b), or $\sigma = \frac{\gamma}{\lambda} > 1$ (Humphries et al., 2006).

Regional properties of functional brain networks

In this study, three nodal parameters, degree (D) (Sporns and Zwi, 2004), nodal efficiency (E_{nod}) (Achard and Bullmore, 2007), and betweenness centrality (BC) (Freeman, 1977), were adopted to characterize the regional properties of the functional networks. Their definitions and descriptions are listed in Table A in the Appendix (see also Rubinov and Sporns, 2010). The nodal characteristics of the brain networks measure the extent to which a given node connects to all other nodes of a network and may indicate the importance of specific brain areas in the network (Achard and Bullmore, 2007; He et al., 2008).

Integrated network parameters

In order to compare condition-related differences of topological properties between brain functional networks regardless of the selection of specific thresholds, we calculated the integrated global parameters of the networks and the integrated regional nodal parameters of node i as summations (Table A; Tian et al., 2011). These integrated regional nodal parameters were used to identify network hubs and to perform further statistical analyses.

Hub identification

Hubs refer to highly connected nodes in a network. In order to determine the hubs in the functional networks, we first calculated the normalized nodal parameter for each node (Table A), then we identified node i as a hub if any of its three nodal parameters NS_{nod} (i) satisfied the criteria (Table A). According to the above description, we determined the hubs of the functional neural networks corresponding to EO and EC, respectively.

Statistical analysis

Network parameters

The integrated network parameters were used for t statistical comparison. Paired t-tests were performed to detect significant differences for any of the six global network parameters ($p < 0.05$) or the three regional nodal parameters ($p < 0.05$, uncorrected) between the EO and EC states.

Inter-regional functional connectivity

To localize the specific connections altered by EO and EC, inter-regional functional connectivity analysis was conducted. To control for the family-wise error rate, we applied a network-based statistic method (NBS; Zalesky et al., 2010a) for the connectivity matrices. A primary cluster-defined threshold ($p = 0.001$) was used to define a set of supra-threshold connections among which any connected component and its size (number of links) were determined. To estimate the significance for each component, we empirically derived the null distribution of connected component size using a nonparametric permutation approach (1000 permutations). For each permutation, the two states (EO and EC) were randomly re-allocated within each subject and a one-tailed, paired t-test was computed independently for each link. Then the same primary threshold ($p = 0.001$) was used to generate supra-threshold links, among which the maximal connected component size was recorded. Finally, for a connected component of size M found in EO/EC, the corrected p-value was determined by finding the proportion of the 1000 permutations for which the maximal connected component was larger than M.

Results

Global properties of the functional brain networks

Because topological properties of the obtained networks are affected by the choice of a specific sparsity value, setting a specific sparsity as the threshold can ensure that the networks corresponding to each subject have the same number of edges. To balance the prominent small-world attribute and the appropriate sparseness in brain functional networks across subjects, we set a series of threshold values for sparsity in the range of 0.10–0.28 at an interval of 0.01. This range of sparsity allows prominent small-world properties in brain networks to be observed (Watts and Strogatz, 1998a).

With the increase of sparsity, both the values of γ and λ decreased monotonically. However, γ is much greater than 1 (Fig. 1C) whereas λ approaches 1 (Fig. 1D) in brain functional networks under EO and EC states. According to Watts and Strogatz (1998b), both of the two sets of networks exhibited small-worldness ($\gamma > 1$ and $\lambda \approx 1$) in the range of $0.10 \le$ sparsity ≤ 0.28. In the present study, we considered only the functional networks in $0.10 \le$ sparsity ≤ 0.28 due to their prominent small-worldness. The network efficiency analysis also demonstrated the small-world configurations ($\frac{E_{loc}^{real}}{E_{loc}^{rand}} > 1$ and $\frac{E_{glob}^{real}}{E_{glob}^{rand}} \approx 1$, Figs. 1G and H) in brain functional networks under EO and EC states.

Paired t-tests revealed significant differences on the integrated global network parameters (C_p, λ, E_{loc} and E_{glob}) between EO and EC ($p < 0.05$, Table 1). Compared to EC, the functional networks under EO showed significantly greater C_p ($t = 3.79$, $p < 0.01$, Figs. 1A and 2), λ ($t = 2.54$, $p < 0.02$, Figs. 1D and 2), and E_{loc} ($t = 4.11$, $p < 0.01$, Figs. 1E and 2), but significantly smaller E_{glob} ($t = -2.10$, $p < 0.05$, Figs. 1F and 2). No significant differences between the two states were found on L_p ($t = 1.95$, $p = 0.06$, Figs. 1B and 2) or γ ($t = 0.37$, $p = 0.71$, Figs. 1C and 2). Given that correlation networks are inherently more clustered than the node and degree matched random networks,

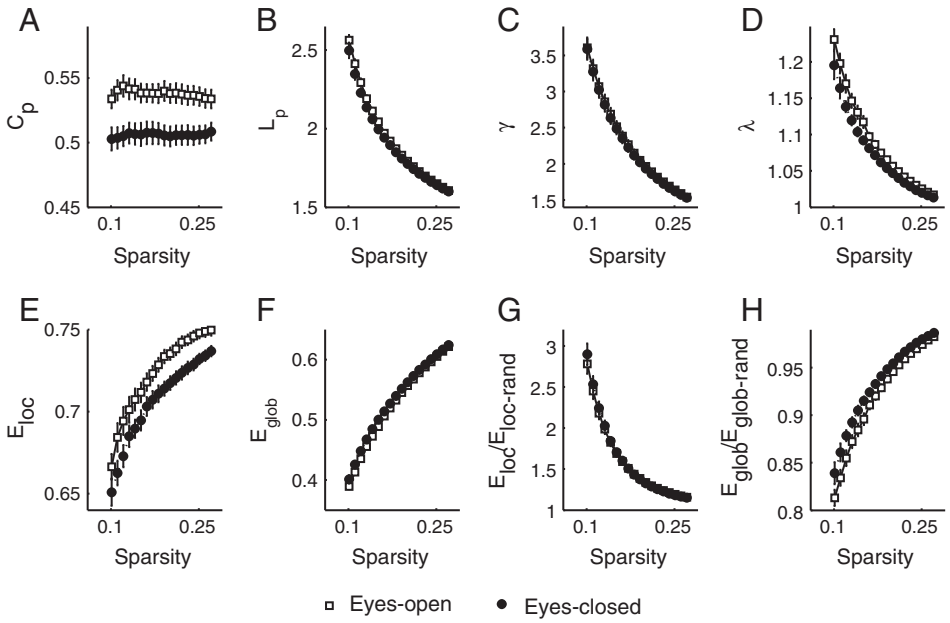

Fig. 1. Topological parameters of the human brain functional networks under eyes-open and eyes-closed changing with the sparsity. The square and circle correspond to the mean value of eyes-open and eyes-closed, respectively, and error bars to the standard error of the subject group in each state. At a wide range of sparsity (0.10–0.28), both of the networks showed $\gamma > 1$ and $\lambda \approx 1$, $E_{loc}/E_{loc\_rand} > 1$, and $E_{glob}/E_{glob\_rand} \approx 1$, which implies that the functional networks exhibit small-world properties. Abbreviations: C_p, clustering coefficient; L_p, characteristic path length; γ, normalized clustering coefficient; λ, normalized shortest path length; E_{loc}, local efficiency; E_{glob}, global efficiency.

the H–Q–S algorithm revealed that the differences between eyes-open and eyes-closed on γ was significant ($t = 3.77, p < 0.01$) but differences in λ were not significant ($t = 1.21, p = 0.24$).

Regional properties of the functional brain networks

Hub regions

Based on the three regional nodal parameters, *D*, E_{nod}, and *BC*, we found ten common hubs shared in functional networks corresponding to both EO and EC. These common hubs mainly include regions belonging to the arousal system (bilateral insula (INS), bilateral rolandic operculum (ROL), and right thalamus (THA.R) (Critchley, 2004; Critchley et al., 2011)), and motor system (right precentral gyrus (PreCG.R) and right supplementary motor area (SMA.R)) (Rizzolatti and Luppino, 2001), somatosensory system (right postcentral gyrus (PoCG.R)) (Fox et al., 1987), and other regions such as bilateral superior temporal gyrus (STG) (Fig. 3A; Table S2). These ten common hubs for EO and EC are indicated by green spheres. In addition, twelve hubs specific to the functional networks of EO were detected, represented by the red color spheres in Fig. 3A. These hub regions were mainly located in regions related to the oculomotor system (PreCG.L) (Nobre et al., 1997), attentional system (left superior parietal gyrus (SPG.L), left inferior parietal lobule (IPL.L)) (Fan et al., 2005), arousal system (THA.L) (Critchley, 2004), and other regions such as bilateral supramarginal gyrus (SMG), bilateral opercular inferior frontal gyrus (IFGoperc), left medial superior frontal gyrus (SFGmed.L), left middle temporal gyrus (MTG.L), right inferior temporal gyrus (ITG.R), and right inferior orbitofrontal cortex (ORBinf.R). We also identified eleven hubs specific to the functional networks of EC, which are shown as blue color spheres in Fig. 3B (Table S2). These eleven hubs were mainly located in the visual system (left lingual gyrus (LING.L), right fusiform gyrus (FFG.R)) (Van Essen, 1979), somatosensory system (PoCG.L) (Fox et al., 1987), part of the default mode network (bilateral anterior cingulate gyrus (ACG), and right angular gyrus (ANG.R)) (Raichle et al., 2001; Van Dijk et al., 2010), and other regions such as bilateral superior temporal pole (TPOsup), bilateral middle frontal gyrus (MFG), right caudate (CAU.R).

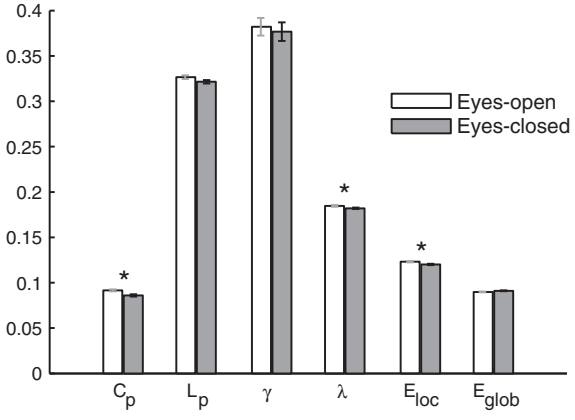

Fig. 2. Integrated global parameters of the brain functional networks corresponding to eyes-open (EO) and eye-closed (EC). Compared to EC, the values of C_p ($p = 0.001$), λ ($p = 0.019$), and E_{loc} ($p < 0.001$) were significantly higher, while the value of E_{glob} ($p = 0.048$) was significantly lower in EO. The symbol '*' indicates a significant difference in the global parameter between the two states.

Table 1
Significant differences in integrated global network parameters between eyes-open and eyes-closed revealed by the paired *t*-test.

	Eyes open	Eyes closed	Eyes open–eyes closed	
	Mean ± SD	Mean ± SD	*t*-Value	*p*-Value
C_p	0.091 ± 0.005	0.086 ± 0.006	**3.789**	**0.001**
L_p	0.327 ± 0.009	0.322 ± 0.009	1.953	0.064
γ	0.382 ± 0.047	0.377 ± 0.049	0.372	0.714
λ	0.185 ± 0.004	0.182 ± 0.004	**2.544**	**0.019**
E_{loc}	0.123 ± 0.003	0.120 ± 0.004	**4.112**	**0.000**
E_{glob}	0.090 ± 0.002	0.091 ± 0.002	**−2.095**	**0.048**

Note: C_p, L_p, γ, λ, E_{loc} and E_{glob} denote the clustering coefficient, characteristic path length, normalized clustering coefficient, normalized shortest path length, local efficiency, and global efficiency, respectively. Significant effects ($p < 0.05$) are indicated by bold text. With the Hirschberger–Qi–Steuer (H–Q–S) algorithm, the differences between eyes-open and eyes-closed in γ was significant ($t = 3.767, p = 0.001$) and on λ was not significant ($t = 1.206, p = 0.241$).

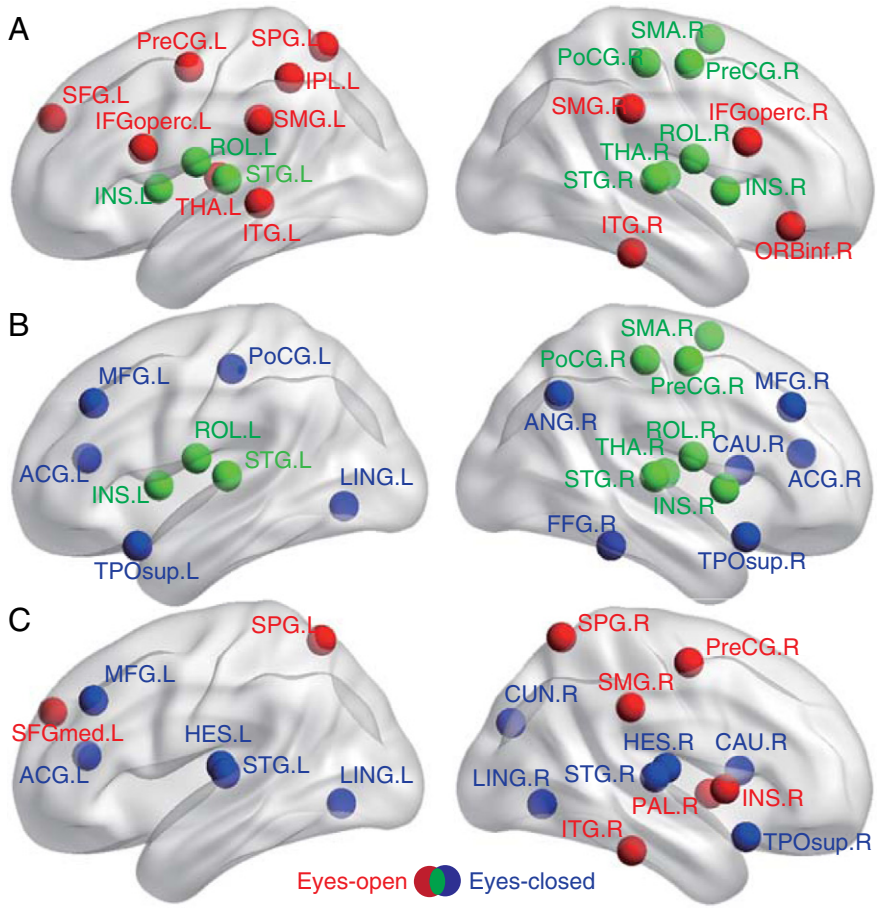

Fig. 3. Plots of nodal characteristics of functional neural networks rendered on the cortical surface. (A) Hub regions of the functional neural networks under eyes-open. The spheres in red indicate the hub regions specific to eyes-open, and those in green indicate the hub region shared in both eyes-open and eyes-closed. (B) Hub regions of the functional neural networks under eyes-closed. The spheres in blue indicate the hub regions specific to eyes-closed, and those in green indicate the hub region shared in both eyes-open and eyes-closed. (C) Brain regions showing significant differences in the integrated regional nodal parameters between eyes-open and eyes-closed. The spheres in red (blue) indicate the regions with significant higher (lower) value of nodal parameters (degree, or nodal efficiency, or betweenness centrality) under eyes-open compared with eyes-closed. The threshold was $p < 0.05$ (uncorrected). Nodes are mapped onto the cortical surfaces using BrainNet Viewer software (Xia et al., 2013).

Differences of nodal characteristics between EO and EC

Paired *t*-tests showed that eight brain regions exhibited significantly increased integrated nodal parameters (D, E_{nod}, or B) in the EO compared to EC ($p < 0.05$, uncorrected). These brain regions were mainly located in the oculomotor system (PreCG.R), attentional system (bilateral SPG) (Corbetta and Shulman, 2002; Fox et al., 2005, 2006), arousal system (INS.R) (Craig, 2009) and other regions such as ITG.R, SMG.R, SFGmed.L, and right pallidum (PAL.R) (red spheres, Fig. 3C; Table S3). Meanwhile, we also found that eleven brain regions showed significant increased integrated nodal parameters (D, E_{nod}, and BC) in EC compared to EO ($p < 0.05$, uncorrected). These brain regions were mainly involved with the visual system (bilateral LING, right cuneus (CUN.R)), auditory system (bilateral Heschl's gyrus (HES)) (Binder et al., 1994; Nobre et al., 1997), part of the default mode network (ACG.L) (Raichle et al., 2001; Van Dijk et al., 2010), and other regions (bilateral STG, CAU.R, MFG.L, and TPOsup.R) (blue spheres, Fig. 3C; Table S3).

Inter-regional functional connectivity

The network-based statistical method (NBS) revealed that 20 connections were significantly more correlated but 51 connections were significantly less correlated under EO than under EC (Fig. 4; Table S4). One-tailed paired *t*-tests revealed three patterns of connectivity corresponding to EO > EC: positive correlations in both EO and EC, negative correlations in both EO and EC, positive correlations in EO but negative correlations in EC. Similar patterns were found in EO < EC. Compared to EC, specifically, the more correlated connections under EO included seven increased positive connections, two decreased negative connections, and six connections positive in EO but negative in EC. These increased connections included five within the visual system and two between visual and attention systems. The two decreased negative connections were located between language (Friederici et al., 2003) and motor systems. The six connections that were positive in EO but negative in EC consisted of two between visual and arousal systems, two between visual and subcortical regions, one between visual and language systems, and one between visual and emotion systems (Bechara et al., 2000). Additionally, the lower correlated connections under EO compared to EC included eleven decreased positive connections and forty negative connections in EO but positive in EC. The decreased positive connections included three between visual and somatosensory systems, five between visual and motor systems, two between visual and auditory systems (Celesia, 1976; Howard et al., 2000), and one between visual and language systems. The negative connections in EO but positive in EC included ten between visual and motor systems, thirteen between visual and somatosensory systems, thirteen between visual and auditory systems, and one between visual and language systems.

Discussion

Although previous studies have attempted to investigate different neural presentations of exteroceptive and interoceptive states by manipulating the orientation of attention (Farb et al., 2013; Simmons

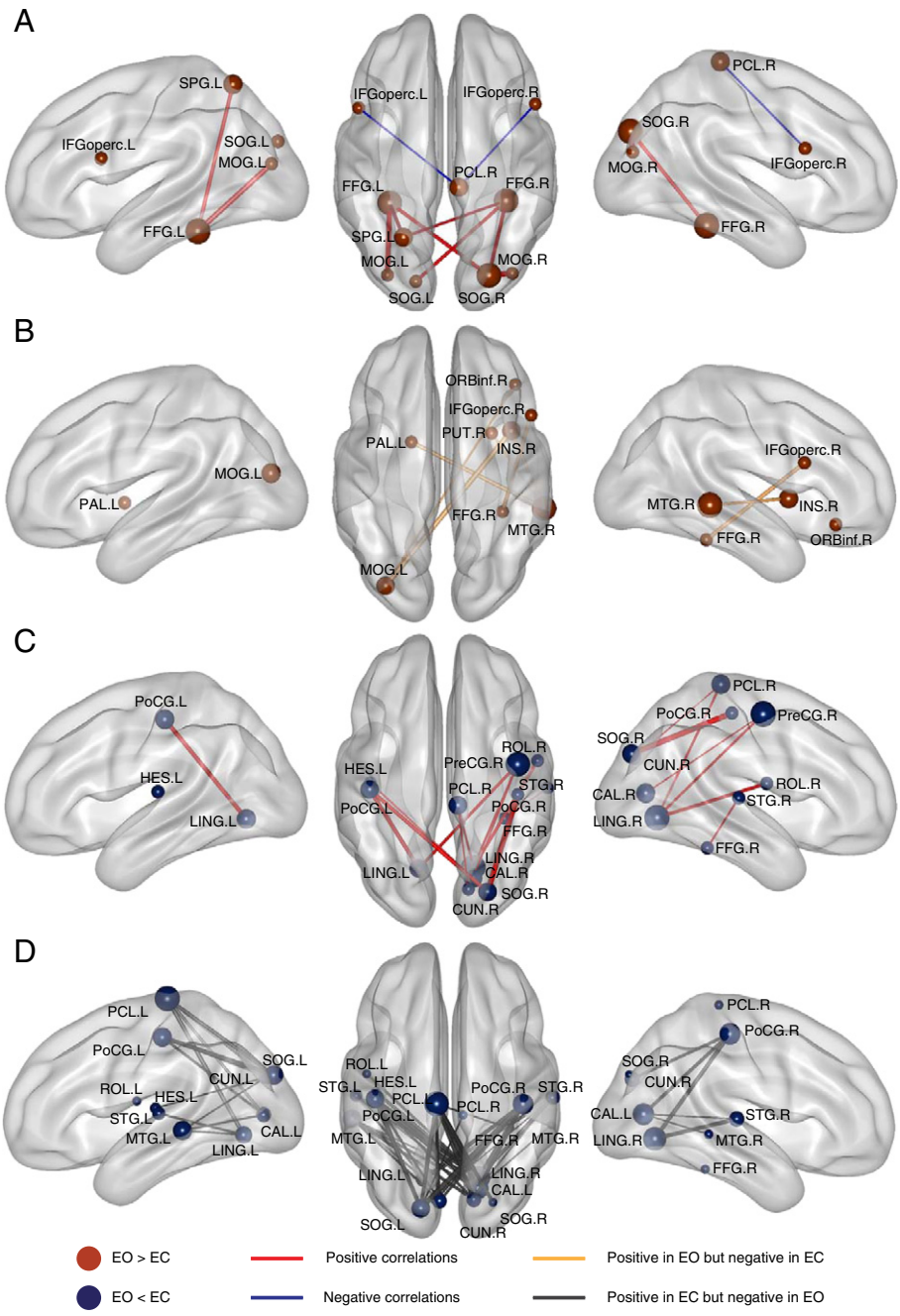

Fig. 4. Plots of the inter-regional functional connections showing significant differences between eyes-open (EO) and eyes-closed (EC). (A) EO > EC, positive (in red) and negative (in blue) correlations for EO compared to EC. (B) EO > EC, correlations that are positive in EO but negative in EC. (C) EO < EC, positive correlations in both EO and EC. (D) EO < EC, correlations that are negative in EO but positive in EC. The nodal size is proportional to the number of links of the node, and the line width was proportional to *t*-value of the connection. Nodes and connections are mapped onto the cortical surfaces using BrainNet Viewer software (Xia et al., 2013).

et al., 2014), the easiest way to control the direction of visual attention as well as balances task difficulty, is simply eyes opened versus eyes closed, an approach which has been largely overlooked. Although previous fMRI studies have found different influences of EO and EC on regional brain activity (Marx et al., 2003, 2004; Wiesmann et al., 2006; Yang et al., 2007) and functional connectivity (Van Dijk et al., 2010; Yan et al., 2009; Zou et al., 2009), the topological organizations of the whole brain networks and the corresponding information processing modes underlying these two states had not yet been identified.

Given that the small-world model supports both specialized and integrated information processing in the brain (Bassett and Bullmore, 2006; Sporns et al., 2004), we adopted graph theoretical approaches to investigate the organizations of brain networks under exteroceptive and interoceptive states with the manipulation of EO and EC. Our results showed that the brain functional networks for both EO and EC exhibited small-world properties, which supported recent findings of brain networks (for a review, see Wang et al., 2010). Thus, this study provided further evidence that functional brain networks exhibit robust small-world properties regardless of the selection of resting conditions, eyes-closed or eyes-open. More importantly, we provided evidence that the topological organizations corresponding to information processing modes of the human brain under the exteroceptive and interoceptive states are somewhat different; there are both domain-general and domain-specific nodes. The domain-specific nodes seem to relate

to specialization of information processing and integration of information processing.

Increased specialized information processing in EO relative to increased integrated information processing in EC

There are two major information processing modes in the functional organization of the brain: specialized information processing and integrated information processing, which serve to generate and integrate information from external and internal sources, respectively (Friston, 2002; Tononi et al., 1998; Zeki and Shipp, 1988). Since information processing occurs in real time (Sporns and Kötter, 2004), this study explored how the characteristic features and efficiency of the two primary information processing modes might be altered if afferent visual information was attenuated by closing the eyes.

Consistent with a previous R-MRI study which found higher regional spontaneous activities in EO (Yan et al., 2009), our results showed higher C_p and E_{loc}, which represents increased specialized information processing when the eyes are open. This suggests that during EO, non-specific or non-goal-directed information may be gathered and evaluated in the brain automatically (Yan et al., 2009). Similar to previous findings of EEG desynchronization (Barry et al., 2007; Chen et al., 2008), we also found higher λ and lower E_{glob} in EO, which indicated the reduced integrated information processing of the functional networks. The connectivity findings further revealed that increased specialized information processing, but decreased integrated information processing pattern in the EO, may result from more specific connections within the visual system (such as MOG.R-SOG.R) and less connections between systems (such as the connection between visual and somatosensory systems (e.g., LING-PreCG.R)) under EO relative to EC. The efficiency of information processing under EC may be disturbed or suppressed by EO (Niven and Laughlin, 2008), which reflects the higher functional specialization of EO (Nir et al., 2006). Our findings demonstrate that there is a modulation of increased specialized information processing but decreased integrated information processing from EC to EO, underlying the shift from interoceptive towards exteroceptive state.

Interoceptive network in EO and exteroceptive network in EC

As previously proposed (Marx et al., 2003), there are two mental states at opposite extremes of one another, an "exteroceptive" state characterized by attention and oculomotor system activity under the EO state, and an "interoceptive" state characterized by imagination and multisensory integration under the EC state (Hufner et al., 2009; Marx et al., 2004; Wiesmann et al., 2006). Our findings, which add evidence based on the nodal properties of neural networks, further support this proposition that there are two distinct networks underlying these two states. One is the "exteroceptive" network, composed of the oculomotor system (PreCG and SFG), attentional system (SPG and IPL) (Corbetta and Shulman, 2002; Fox et al., 2005, 2006), and the arousal system (INS, ROL and THA) (Critchley, 2004; Critchley et al., 2011). This network is specific to EO, underlying the exteroceptive state for alertness and readiness (Fransson, 2005; McAvoy et al., 2008). The other is the "interoceptive" network, which mainly includes the visual system (LING., FFG, and STG), auditory system (HES), somatosensory system (PoCG), and part of the default mode network (ANG and ACG) (Raichle et al., 2001; Van Dijk et al., 2010). This network is specific to EC, underlying introspective state for imagination and recall of sensory experiences (Hufner et al., 2009; Marx et al., 2003).

The present findings were consistent with previous investigations in showing that both the activation of the visual system (mainly including the extrastriate body area, such as LING) (Bianciardi et al., 2009; Hufner et al., 2008, 2009; Marx et al., 2003, 2004) and the connections between visual (mainly including the extrastriate body area) and motor system (such as LING-PreCG.R) (Nir et al., 2006; Wiesmann et al., 2006; Zou et al., 2009) are attenuated under EO compared to EC. Given that the extrastriate body area (such as LING) and premotor cortex (such as PreCG) are associated with body identity and body actions, respectively (Astafiev et al., 2004; Downing et al., 2001; Urgesi et al., 2007), one possible interpretation is that the subjects were imagining body motion during the suppression of natural urges in EC.

Cross-sensory modality connections are altered in EO/EC

Stronger coupling of the visual system with motor, somatosensory and auditory system may indicate high synchronization across sensory modalities during EC. Given that LING and FFG are believed to play an important role in visual imagery and memory (Bogousslavsky et al., 1987; Machielsen et al., 2000), this higher coupling may be the result of non-specific imagination leading to the recall of sensory experiences during EC (Damasio, 1996; Marx et al., 2003). This cross-modality synchronism was attenuated and the connections among visual and attention, arousal, and subcortical systems were increased with eyes opening; this may indicate that EO leads to a suppression of sensory modalities other than vision to capture more resources and energy for exteroceptive processing (Bianciardi et al., 2009; Niven and Laughlin, 2008). These connectivity findings, consistent with network metrics, further suggest a switch in information processing mode from highly integrated (EC) to highly specialized (EO).

It is worth mentioning that a recent study reported no evidence of differences in topological organization of brain functional networks between EO and EC (Jao et al., 2013). They did find widespread differences between EO and EC on the spontaneous activity and functional connectivity of brain, but there were no apparent differences on whole brain topological organization other than the connection distance, an index of the information processing of a network (Sepulcre et al., 2010), between EO and EC. Possible explanations for the discrepancy between these two studies are as follows: (1) GSR was used in the present study but not the previous one, (2) the parcellation templates were different, and (3) the spatial resolutions were different (data acquisition parameters).

Global variations of the BOLD signal are often considered nuisance effects and are commonly removed as a covariate in a regression model. Thus, GSR is widely used to remove noise generated by the scanner (such as signal drifting and spikes). There is much debate about its utility in fMRI data pre-processing (Chai et al., 2012a; Fox et al., 2009; Murphy et al., 2009; Weissenbacher et al., 2009), because it centers the distribution of correlations around zero and may introduce spurious correlations (Saad et al., 2012). The concern is especially relevant when interpreting negative correlations, since they may be solely the result of GSR, rather than reflecting true neuronal activation/deactivation (Murphy et al., 2009). Though, it is worth noting that recent electrophysiological work indicates wide-spread positive correlations across nearly the entire cortex (Scholvinck et al., 2010). These wide-spread correlations may require mitigation to examine local network properties. Additionally, recent work examining the impact of standardization procedures (e.g., GSR and mean subtraction) for motion artifacts on connectivity patterns, suggests that some normalization procedure (e.g., GSR) is better than none (e.g., no GSR) (Yan et al., 2013). Given these issues, we analyzed the data both with and without GSR. Our results showed that differences in negative correlations disappeared without GSR, but the pattern of main results and conclusion remained (Supplementary materials). Compared with results without GSR, our results with GSR were more consistent with previous results (Hufner et al., 2008; Marx et al., 2003, 2004; Nir et al., 2006; Wiesmann et al., 2006). That is, our results with GSR were more sensitive to the differences between EO and EC compared to those obtained without GSR, which is also in consistent with the results of Fox et al. (2009). Therefore, GSR is one possible reason for the discrepancy between our findings and those of Jao et al. (2013).

Given the important impact of different parcellation strategies (especially the spatial scale of the nodal parcellation) on topological parameters (e.g. small-worldness and efficiency) of functional brain networks (Power et al., 2011; Wang et al., 2009; Wig et al., 2011; Zalesky et al., 2010b), another potential explanation for the current discrepancy is the different parcellation templates. Although the topological parameters vary considerably as a function of spatial nodal scale (Zalesky et al., 2010b), it is hard to identify a specific nodal scale that maximize sensitivity to differences of topological organizations between conditions. For example, lower spatial resolution enhances signal-to-noise ratio of the time series at each region, which in turn adds noise to the inter-regional connectivity matrix. One possible explanation is that the sub-sampling of the anatomically based AAL template disturbs both intra- and inter-regional connections, which reduced the sensitivity to test the differences between EO and EC by Jao et al. (2013). Another explanation is that the higher spatial resolution in data acquisition increased the sensitivity in our study. These two possibilities are not mutually exclusive. Building on Jao et al.'s (2013) findings, the present study uses a more sensitive parcellation template and higher spatial resolution, which may further clarify the influence of volitional eye opening on the spontaneous activity of the brain. Taken together, volitional eye opening influences not only the spontaneous activity of the isolated brain regions and the inter-regional function connectivity, but also the functional integration of multiple brain regions and whole brain topological organizations.

Although EO and EC correspond to exteroceptive and interoceptive states respectively (Marx et al., 2003) and these correspondences are supported by both the current results and previous findings (Bianciardi et al., 2009; Brandt, 2006; Hufner et al., 2008, 2009; Marx et al., 2004; McAvoy et al., 2008, 2012; Niven and Laughlin, 2008), it potentially oversimplifies the relationship between EO/EC and exteroceptive/interoceptive states. We can neither argue that interoceptively oriented attention is absent under EO (Farb et al., 2013), nor that exteroceptively oriented attention is absent under EC (Fransson, 2005). More elaborate manipulations of attentional orientation should be conducted in the future to address this question (Farb et al., 2013; Simmons et al., 2014). Since skin conductance is a sensitive psychophysiological index of bodily state (Critchley, 2002; Critchley et al., 2004) and is highly correlated with spontaneous brain activity (Fan et al., 2012), skin conductance indices could shed further light on interoceptive and exteroceptive processing.

In summary, EO and EC were evaluated during resting state, without any top-down attentional manipulation, such as visual fixation (Bianciardi et al., 2009; Yang et al., 2007) or attentional orientation (Farb et al., 2013; Simmons et al., 2014). Thus, the only differences between EO and EC were visual sensory information and subjective/objective state characteristics of EO and EC. Therefore, we speculate that the eyes act as a toggle between an exteroceptive network and interoceptive network rather than simply a gate of visual sensory information (Burton et al., 2004; Hufner et al., 2009). Having the eyes open or closed modulates a shift between prominently exteroceptive network activity and prominently interoceptive network activity, respectively. This shift, from EO to EC also corresponds to an information processing mode of more specialized towards more integrated. Taking into account the wide applicability of the R-fMRI and graph-based analysis to various studies, our findings also suggested that the choice of the resting condition (either eyes closed or eyes open) is an important factor to be carefully considered given different research objectives.

Acknowledgments

This work was supported by the Natural Science Foundation of China (Grant numbers: 91132704, 81071149, 81030028, 81271548, and 81371535), the National Basic Research Program of China (973 Program, 2011CB711000, 2014CB744600), the National Science Fund for Distinguished Young Scholars (Grant number: 81225012), and Scientific Research Foundation for the Returned Overseas Chinese Scholars (RH), and State Education Ministry of China. We thank Alexander Dufford for offering helpful comments.

Conflict of interest

The authors declare no competing financial interests.

Appendix A

Table A
Expressions and descriptions of the network parameters applied in this study.

Network parameters	Definitions	Descriptions
Clustering coefficient (C_p)	$C_P = \frac{1}{N}\sum_{i\in G}\frac{K_i}{D(i)(D(i)\text{-}1)/2}$	C_p measures the local cliquishness of a network G with N nodes and K edges. K_i is the number of edges in G (i), the subgraph consisting of the neighbors of node i.
Characteristic path length (L_p)	$L_p = \frac{1}{\frac{1}{N(N-1)}\sum_{j\neq i\in G}\frac{1}{L_{ij}}}$	L_p measures the overall routing efficiency of the network. L_{ij} is the shortest path length between nodes i and j.
Global efficiency (E_{glob})	$E_{glob} = \frac{1}{N(N-1)}\sum_{j\neq i\in G}\frac{1}{L_{ij}}$	E_{glob} measures the extent of information propagation through the whole network.
Local efficiency (E_{loc})	$E_{loc} = \frac{1}{N}\sum_{i\in G}E_{glob}(i)$	E_{loc} measures the mean local efficiency of the network.
Degree (D)	$D(i) = \sum_{j\neq i\in G} e_{ij}$	D (i) measures the connectivity of node i with the rest of the nodes in a network, e_{ij} is the (i, j)th element in the formerly obtained binarized correlation matrix.
Efficiency (E_{nod})	$E_{nod}(i) = \frac{1}{N\text{-}1}\sum_{j\neq i\in G}\frac{1}{L_{ij}}$	E_{nod} (i) measures the ability of information transmission of node i in the network.
Betweenness centrality (BC)	$BC(i) = \sum_{j\neq i\neq k\in G}\frac{\delta_{jk}(i)}{\delta_{jk}}$	BC (i) measures the influence of node i over information flow between other nodes in the whole network. δ_{jk} is the number of the shortest paths from node j to node k, and δ_{jk} (i) is the number of the shortest paths from node j to node k that pass through node i within the network G.
Integrated global parameters (S_{glob})	$S_{glob} = \sum_{k=10}^{28} S(k\bullet\Delta s)\Delta s$	S_{glob} measures the area under curve (AUC) of each global network parameter (C_p, L_p, γ, λ, E_{glob}, and E_{loc}). S ($k\cdot\Delta s$) represents any of the global parameters at the sparsity of $k\cdot\Delta s$, and Δs is the sparsity interval of 0.01. The range of sparsity was selected from 0.01 to 0.28 ($0.01 \le k \le 0.28$, see the Results section) in the current study.
Integrated nodal parameters (S_{nod})	$S_{nod}(i) = \sum_{k=10}^{28} S(i, k\Delta s)\Delta s$	S_{nod} measures the AUC of each nodal parameter (D, E_{nod}, and BC). S (i, $k\cdot\Delta s$) represents any of the nodal parameters of the node i at a sparsity of $k\cdot\Delta s$.
Normalized nodal parameters (NS_{nod})	$NS_{nod}(i) = \frac{N\cdot\sum_{k=1}^{M} S_{nod}(i,k)}{\sum_{j=1}^{N}\sum_{k=1}^{M} S_{nod}(j,k)}$	NS_{nod} is the normalized integrated nodal parameters. S_{nod} (i, k) represents one of these three integrated nodal parameters (D, E_{nod}, and BC) at node i for the network of subject k; N is the number of nodes and M is the number of subjects.
Hub identification criterion	$NS_{nod}(i) > \text{mean}(S) + \text{SD}$	The criterion to identify the hub. The mean (S) stands for the averaged value of NS_{nod} (i), and SD for the standard deviation of NS_{nod} (i) across all nodes of the network.

Appendix B. Supplementary data

Supplementary data to this article can be found online at http://dx.doi.org/10.1016/j.neuroimage.2013.12.060.

References

Achard, S., Bullmore, E., 2007. Efficiency and cost of economical brain functional networks. PLoS Comput. Biol. 3, 174–183.

Astafiev, S.V., Stanley, C.M., Shulman, G.L., Corbetta, M., 2004. Extrastriate body area in human occipital cortex responds to the performance of motor actions. Nat. Neurosci. 7, 542–548.

Barry, R.J., Clarke, A.R., Johnstone, S.J., Magee, C.A., Rushby, J.A., 2007. EEG differences between eyes-closed and eyes-open resting conditions. Clin. Neurophysiol. 118, 2765–2773.

Bassett, D.S., Bullmore, E., 2006. Small-world brain networks. Neuroscientist 12, 512–523.

Bechara, A., Damasio, H., Damasio, A.R., 2000. Emotion, decision making and the orbitofrontal cortex. Cereb. Cortex 10, 295–307.

Bianciardi, M., Fukunaga, M., van Gelderen, P., Horovitz, S.G., de Zwart, J.A., Duyn, J.H., 2009. Modulation of spontaneous fMRI activity in human visual cortex by behavioral state. Neuroimage 45, 160–168.

Binder, J.R., Rao, S.M., Hammeke, T.A., Yetkin, F.Z., Jesmanowicz, A., Bandettini, P.A., Wong, E.C., Estkowski, L.D., Goldstein, M.D., Haughton, V.M., Hyde, J.S., 1994. Functional magnetic-resonance-imaging of human auditory-cortex. Ann. Neurol. 35, 662–672.

Bogousslavsky, J., Miklossy, J., Deruaz, J.P., Assal, G., Regli, F., 1987. Lingual and fusiform gyri in visual processing: a clinico-pathologic study of superior altitudinal hemianopia. J. Neurol. Neurosurg. Psychiatry 50, 607–614.

Brandt, T., 2006. How to see what you are looking for in fMRI and PET — or the crucial baseline condition. J. Neurol. 253, 551–555.

Bullmore, E., Sporns, O., 2009. Complex brain networks: graph theoretical analysis of structural and functional systems. Nat. Rev. Neurosci. 10, 186–198.

Burton, H., Snyder, A.Z., Raichle, M.E., 2004. Default brain functionality in blind people. Proc. Natl. Acad. Sci. U. S. A. 101, 15500–15505.

Celesia, G.G., 1976. Organization of auditory cortical areas in man. Brain 99, 403–414.

Chai, X.J., Castanon, A.N., Ongur, D., Whitfield-Gabrieli, S., 2012a. Anticorrelations in resting state networks without global signal regression. Neuroimage 59, 1420–1428.

Chai, X.Q.J., Castanon, A.N., Ongur, D., Whitfield-Gabrieli, S., 2012b. Anticorrelations in resting state networks without global signal regression. Neuroimage 59, 1420–1428.

Chen, A.C., Feng, W., Zhao, H., Yin, Y., Wang, P., 2008. EEG default mode network in the human brain: spectral regional field powers. Neuroimage 41, 561–574.

Corbetta, M., Shulman, G.L., 2002. Control of goal-directed and stimulus-driven attention in the brain. Nat. Rev. Neurosci. 3, 201–215.

Craig, A.D., 2009. How do you feel—now? The anterior insula and human awareness. Nat. Rev. Neurosci. 10, 59–70.

Crick, F., Koch, C., 2003. A framework for consciousness. Nat. Neurosci. 6, 119–126.

Critchley, H.D., 2002. Electrodermal responses: what happens in the brain. Neuroscientist 8, 132–142.

Critchley, H.D., 2004. The human cortex responds to an interoceptive challenge. Proc. Natl. Acad. Sci. U. S. A. 101, 6333–6334.

Critchley, H.D., Wiens, S., Rotshtein, P., Ohman, A., Dolan, R.J., 2004. Neural systems supporting interoceptive awareness. Nat. Neurosci. 7, 189–195.

Critchley, H.D., Nagai, Y., Gray, M.A., Mathias, C.J., 2011. Dissecting axes of autonomic control in humans: insights from neuroimaging. Auton. Neurosci. 161, 34–42.

Damasio, A.R., 1996. The somatic marker hypothesis and the possible functions of the prefrontal cortex. Philos. Trans. R. Soc. Lond. B Biol. Sci. 351, 1413–1420.

Downing, P.E., Jiang, Y., Shuman, M., Kanwisher, N., 2001. A cortical area selective for visual processing of the human body. Science 293, 2470–2473.

Fan, J., McCandliss, B.D., Fossella, J., Flombaum, J.I., Posner, M.I., 2005. The activation of attentional networks. Neuroimage 26, 471–479.

Fan, J., Xu, P., Van Dam, N.T., Eilam-Stock, T., Gu, X., Luo, Y.J., Hof, P.R., 2012. Spontaneous brain activity relates to autonomic arousal. J. Neurosci. 32, 11176–11186.

Farb, N.A., Segal, Z.V., Anderson, A.K., 2013. Attentional modulation of primary interoceptive and exteroceptive cortices. Cereb. Cortex 23, 114–126.

Fox, P.T., Burton, H., Raichle, M.E., 1987. Mapping human somatosensory cortex with positron emission tomography. J. Neurosurg. 67, 34–43.

Fox, M.D., Snyder, A.Z., Vincent, J.L., Corbetta, M., Van Essen, D.C., Raichle, M.E., 2005. The human brain is intrinsically organized into dynamic, anticorrelated functional networks. Proc. Natl. Acad. Sci. U. S. A. 102, 9673–9678.

Fox, M.D., Corbetta, M., Snyder, A.Z., Vincent, J.L., Raichle, M.E., 2006. Spontaneous neuronal activity distinguishes human dorsal and ventral attention systems. Proc. Natl. Acad. Sci. U. S. A. 103, 10046–10051.

Fox, M.D., Zhang, D., Snyder, A.Z., Raichle, M.E., 2009. The global signal and observed anticorrelated resting state brain networks. J. Neurophysiol. 101, 3270–3283.

Fransson, P., 2005. Spontaneous low-frequency BOLD signal fluctuations: an fMRI investigation of the resting-state default mode of brain function hypothesis. Hum. Brain Mapp. 26, 15–29.

Freeman, L.C., 1977. A set of measures of centrality based on betweenness. Sociometry 40, 35–41.

Friederici, A.D., Ruschemeyer, S.A., Hahne, A., Fiebach, C.J., 2003. The role of left inferior frontal and superior temporal cortex in sentence comprehension: localizing syntactic and semantic processes. Cereb. Cortex 13, 170–177.

Friston, K., 2002. Beyond phrenology: what can neuroimaging tell us about distributed circuitry? Annu. Rev. Neurosci. 25, 221–250.

Griswold, M.A., Jakob, P.M., Heidemann, R.M., Nittka, M., Jellus, V., Wang, J., Kiefer, B., Haase, A., 2002. Generalized autocalibrating partially parallel acquisitions (GRAPPA). Magn. Reson. Med. 47, 1202–1210.

Hagmann, P., Cammoun, L., Gigandet, X., Meuli, R., Honey, C.J., Wedeen, V.J., Sporns, O., 2008. Mapping the structural core of human cerebral cortex. PLoS Biol. 6, e159.

He, Y., Evans, A., 2010. Graph theoretical modeling of brain connectivity. Curr. Opin. Neurol. 23, 341–350.

He, Y., Chen, Z., Evans, A., 2008. Structural insights into aberrant topological patterns of large-scale cortical networks in Alzheimer's disease. J. Neurosci. 28, 4756–4766.

Howard, M.A., Volkov, I.O., Mirsky, R., Garell, P.C., Noh, M.D., Granner, M., Damasio, H., Steinschneider, M., Reale, R.A., Hind, J.E., Brugge, J.F., 2000. Auditory cortex on the human posterior superior temporal gyrus. J. Comp. Neurol. 416, 79–92.

Hufner, K., Stephan, T., Glasauer, S., Kalla, R., Riedel, E., Deutschlander, A., Dera, T., Wiesmann, M., Strupp, M., Brandt, T., 2008. Differences in saccade-evoked brain activation patterns with eyes open or eyes closed in complete darkness. Exp. Brain Res. 186, 419–430.

Hufner, K., Stephan, T., Flanagin, V.L., Deutschlander, A., Stein, A., Kalla, R., Dera, T., Fesl, G., Jahn, K., Strupp, M., Brandt, T., 2009. Differential effects of eyes open or closed in darkness on brain activation patterns in blind subjects. Neurosci. Lett. 466, 30–34.

Humphries, M.D., Gurney, K., Prescott, T.J., 2006. The brainstem reticular formation is a small-world, not scale-free, network. Proc. Biol. Sci. 273, 503–511.

Jao, T., Vertes, P.E., Alexander-Bloch, A.F., Tang, I.N., Yu, Y.C., Chen, J.H., Bullmore, E.T., 2013. Volitional eyes opening perturbs brain dynamics and functional connectivity regardless of light input. Neuroimage 69, 21–34.

Latora, V., Marchiori, M., 2001. Efficient behavior of small-world networks. Phys. Rev. Lett. 87, 198701.

Machielsen, W.C., Rombouts, S.A., Barkhof, F., Scheltens, P., Witter, M.P., 2000. FMRI of visual encoding: reproducibility of activation. Hum. Brain Mapp. 9, 156–164.

Marx, E., Stephan, T., Nolte, A., Deutschländer, A., Seelos, K.C., Dieterich, M., Brandt, T., 2003. Eye closure in darkness animates sensory systems. Neuroimage 19, 924–934.

Marx, E., Deutschlander, A., Stephan, T., Dieterich, M., Wiesmann, M., Brandt, T., 2004. Eyes open and eyes closed as rest conditions: impact on brain activation patterns. Neuroimage 21, 1818–1824.

Maslov, S., Sneppen, K., 2002. Specificity and stability in topology of protein networks. Science 296, 910–913.

McAvoy, M., Larson-Prior, L., Nolan, T.S., Vaishnavi, S.N., Raichle, M.E., d'Avossa, G., 2008. Resting states affect spontaneous BOLD oscillations in sensory and paralimbic cortex. J. Neurophysiol. 100, 922–931.

McAvoy, M., Larson-Prior, L., Ludwikow, M., Zhang, D., Snyder, A.Z., Gusnard, D.L., Raichle, M.E., d'Avossa, G., 2012. Dissociated mean and functional connectivity BOLD signals in visual cortex during eyes closed and fixation. J. Neurophysiol. 108, 2363–2372.

Milo, R., Shen-Orr, S., Itzkovitz, S., Kashtan, N., Chklovskii, D., Alon, U., 2002. Network motifs: simple building blocks of complex networks. Science 298, 824–827.

Mowinckel, A.M., Espeseth, T., Westlye, L.T., 2012. Network-specific effects of age and in-scanner subject motion: a resting-state fMRI study of 238 healthy adults. Neuroimage 63, 1364–1373.

Murphy, K., Birn, R.M., Handwerker, D.A., Jones, T.B., Bandettini, P.A., 2009. The impact of global signal regression on resting state correlations: are anti-correlated networks introduced? Neuroimage 44, 893–905.

Nakano, T., Kato, M., Morito, Y., Itoi, S., Kitazawa, S., 2013. Blink-related momentary activation of the default mode network while viewing videos. Proc. Natl. Acad. Sci. U. S. A. 110, 702–706.

Newman, M.E.J., 2003. The structure and function of complex networks. SIAM Rev. 45, 167–256.

Nir, Y., Hasson, U., Levy, I., Yeshurun, Y., Malach, R., 2006. Widespread functional connectivity and fMRI fluctuations in human visual cortex in the absence of visual stimulation. Neuroimage 30, 1313–1324.

Niven, J.E., Laughlin, S.B., 2008. Energy limitation as a selective pressure on the evolution of sensory systems. J. Exp. Biol. 211, 1792–1804.

Nobre, A.C., Sebestyen, G.N., Gitelman, D.R., Mesulam, M.M., Frackowiak, R.S.J., Frith, C.D., 1997. Functional localization of the system for visuospatial attention using positron emission tomography. Brain 120, 515–533.

Power, J.D., Cohen, A.L., Nelson, S.M., Wig, G.S., Barnes, K.A., Church, J.A., Vogel, A.C., Laumann, T.O., Miezin, F.M., Schlaggar, B.L., Petersen, S.E., 2011. Functional network organization of the human brain. Neuron 72, 665–678.

Power, J.D., Barnes, K.A., Snyder, A.Z., Schlaggar, B.L., Petersen, S.E., 2012. Spurious but systematic correlations in functional connectivity MRI networks arise from subject motion. Neuroimage 59, 2142–2154.

Raichle, M.E., MacLeod, A.M., Snyder, A.Z., Powers, W.J., Gusnard, D.A., Shulman, G.L., 2001. A default mode of brain function. Proc. Natl. Acad. Sci. U. S. A. 98, 676–682.

Rizzolatti, G., Luppino, G., 2001. The cortical motor system. Neuron 31, 889–901.

Rubinov, M., Sporns, O., 2010. Complex network measures of brain connectivity: uses and interpretations. Neuroimage 52, 1059–1069.

Saad, Z.S., Gotts, S.J., Murphy, K., Chen, G., Jo, H.J., Martin, A., Cox, R.W., 2012. Trouble at rest: how correlation patterns and group differences become distorted after global signal regression. Brain Connect. 2, 25–32.

Satterthwaite, T.D., Wolf, D.H., Loughead, J., Ruparel, K., Elliott, M.A., Hakonarson, H., Gur, R.C., Gur, R.E., 2012. Impact of in-scanner head motion on multiple measures of functional connectivity: relevance for studies of neurodevelopment in youth. Neuroimage 60, 623–632.

Scholvinck, M.L., Maier, A., Ye, F.Q., Duyn, J.H., Leopold, D.A., 2010. Neural basis of global resting-state fMRI activity. Proc. Natl. Acad. Sci. U. S. A. 107, 10238–10243.

Sepulcre, J., Liu, H., Talukdar, T., Martincorena, I., Yeo, B.T., Buckner, R.L., 2010. The organization of local and distant functional connectivity in the human brain. PLoS Comput. Biol. 6, e1000808.

Simmons, W.K., Avery, J.A., Barcalow, J.C., Bodurka, J., Drevets, W.C., Bellgowan, P., 2014. Keeping the body in mind: insula functional organization and functional connectivity integrate interoceptive, exteroceptive, and emotional awareness. Hum. Brain Mapp. 34, 2944–2958.
Sporns, O., Kötter, R., 2004. Motifs in brain networks. PLoS Biol. 2, e369.
Sporns, O., Zwi, J.D., 2004. The small world of the cerebral cortex. Neuroinformatics 2, 145–162.
Sporns, O., Chialvo, D.R., Kaiser, M., Hilgetag, C.C., 2004. Organization, development and function of complex brain networks. Trends Cogn. Sci. 8, 418–425.
Tian, L., Wang, J., Yan, C., He, Y., 2011. Hemisphere- and gender-related differences in small-world brain networks: a resting-state functional MRI study. Neuroimage 54, 191–202.
Tononi, G., Edelman, G.M., Sporns, O., 1998. Complexity and coherency: integrating information in the brain. Trends Cogn. Sci. 2, 474–484.
Tzourio-Mazoyer, N., Landeau, B., Papathanassiou, D., Crivello, F., Etard, O., Delcroix, N., Mazoyer, B., Joliot, M., 2002. Automated anatomical labeling of activations in SPM using a macroscopic anatomical parcellation of the MNI MRI single-subject brain. Neuroimage 15, 273–289.
Urgesi, C., Candidi, M., Ionta, S., Aglioti, S.M., 2007. Representation of body identity and body actions in extrastriate body area and ventral premotor cortex. Nat. Neurosci. 10, 30–31.
Van Dijk, K.R., Hedden, T., Venkataraman, A., Evans, K.C., Lazar, S.W., Buckner, R.L., 2010. Intrinsic functional connectivity as a tool for human connectomics: theory, properties, and optimization. J. Neurophysiol. 103, 297–321.
Van Dijk, K.R., Sabuncu, M.R., Buckner, R.L., 2012. The influence of head motion on intrinsic functional connectivity MRI. Neuroimage 59, 431–438.
Van Essen, D.C., 1979. Visual areas of the mammalian cerebral cortex. Annu. Rev. Neurosci. 2, 227–263.
Wang, J., Wang, L., Zang, Y., Yang, H., Tang, H., Gong, Q., Chen, Z., Zhu, C., He, Y., 2009. Parcellation-dependent small-world brain functional networks: a resting-state fMRI study. Hum. Brain Mapp. 30, 1511–1523.
Wang, J., Zuo, X., He, Y., 2010. Graph-based network analysis of resting-state functional MRI. Front. Syst. Neurosci. 4, 16.
Watts, D.J., Strogatz, S.H., 1998a. Collective dynamics of 'small-world' networks. Nature 393, 440–442.
Watts, D.J., Strogatz, S.H., 1998b. Collective dynamics of'small-world'networks. Nature 393, 440–442.
Weissenbacher, A., Kasess, C., Gerstl, F., Lanzenberger, R., Moser, E., Windischberger, C., 2009. Correlations and anticorrelations in resting-state functional connectivity MRI: a quantitative comparison of preprocessing strategies. Neuroimage 47, 1408–1416.
Wiesmann, M., Kopietz, R., Albrecht, J., Linn, J., Reime, U., Kara, E., Pollatos, O., Sakar, V., Anzinger, A., Fesl, G., Bruckmann, H., Kobal, G., Stephan, T., 2006. Eye closure in darkness animates olfactory and gustatory cortical areas. Neuroimage 32, 293–300.
Wig, G.S., Schlaggar, B.L., Petersen, S.E., 2011. Concepts and principles in the analysis of brain networks. Ann. N. Y. Acad. Sci. 1224, 126–146.
Xia, M., Wang, J., He, Y., 2013. BrainNet Viewer: a network visualization tool for human brain connectomics. PLoS One 8, e68910.
Yan, C.-G., Zang, Y.-F., 2010. DPARSF: a MATLAB toolbox for "pipeline" data analysis of resting-state fMRI. Front. Syst. Neurosci. 4, 13.
Yan, C., Liu, D., He, Y., Zou, Q., Zhu, C., Zuo, X., Long, X., Zang, Y., 2009. Spontaneous brain activity in the default mode network is sensitive to different resting-state conditions with limited cognitive load. PLoS One 4, e5743.
Yan, C.G., Craddock, R.C., Zuo, X.N., Zang, Y.F., Milham, M.P., 2013. Standardizing the intrinsic brain: towards robust measurement of inter-individual variation in 1000 functional connectomes. Neuroimage 80, 246–262.
Yang, H., Long, X.Y., Yang, Y., Yan, H., Zhu, C.Z., Zhou, X.P., Zang, Y.F., Gong, Q.Y., 2007. Amplitude of low frequency fluctuation within visual areas revealed by resting-state functional MRI. Neuroimage 36, 144–152.
Zalesky, A., Fornito, A., Bullmore, E.T., 2010a. Network-based statistic: identifying differences in brain networks. Neuroimage 53, 1197–1207.
Zalesky, A., Fornito, A., Harding, I.H., Cocchi, L., Yucel, M., Pantelis, C., Bullmore, E.T., 2010b. Whole-brain anatomical networks: does the choice of nodes matter? Neuroimage 50, 970–983.
Zalesky, A., Fornito, A., Bullmore, E., 2012. On the use of correlation as a measure of network connectivity. Neuroimage 60, 2096–2106.
Zeki, S., Shipp, S., 1988. The functional logic of cortical connections. Nature 335, 311–317.
Zou, Q., Long, X., Zuo, X., Yan, C., Zhu, C., Yang, Y., Liu, D., He, Y., Zang, Y., 2009. Functional connectivity between the thalamus and visual cortex under eyes closed and eyes open conditions: a resting-state fMRI study. Hum. Brain Mapp. 30, 3066–3078.
Zuo, X.N., Xu, T., Jiang, L., Yang, Z., Cao, X.Y., He, Y., Zang, Y.F., Castellanos, F.X., Milham, M.P., 2013. Toward reliable characterization of functional homogeneity in the human brain: preprocessing, scan duration, imaging resolution and computational space. Neuroimage 65, 374–386.